Vibrational density of states in silicon carbide nanoparticles: experiments and numerical simulations

2005 J. Phys.: Condens. Matter 17 5101

(http://iopscience.iop.org/0953-8984/17/33/014)

INSTITUTE OF PHYSICS PUBLISHING JOURNAL OF PHYSICS: CONDENSED MATTER

J. Phys.: Condens. Matter **17** (2005) 5101–5110 doi:10.1088/0953-8984/17/33/014

Vibrational density of states in silicon carbide nanoparticles: experiments and numerical simulations

M Makowska-Janusik[1], A Kassiba[2,5], J Bouclé[2,3], J-F Bardeau[2], S Kodjikian[4] and A Désert[2]

[1] Institute of Physics, Jan Dlugosz University, Al Armii Krajowej 13/15, PL-42201 Częstochowa, Poland
[2] Laboratoire de Physique de l'Etat Condensé, UMR-CNRS 6087, Université du Maine, Avenue Olivier Messiaen—72085 Le Mans Cedex 9, France
[3] Laboratoire Francis Perrin—Service des Photons, Atomes et Molécules, CEA-CNRS URA 2453-CEA/DSM, Saclay 91191 Gif sur Yvette Cedex, France
[4] Laboratoire des Fluorures, UMR-CNRS 6010, Université du Maine, 72085 Le Mans Cedex 9, France

E-mail: kassiba@univ-lemans.fr

Received 3 February 2005, in final form 18 May 2005
Published 5 August 2005
Online at stacks.iop.org/JPhysCM/17/5101

Abstract

The vibrational properties of silicon carbide nanoparticles (np-SiC) were investigated as function of the nanocrystal size (5–25 nm) and the features of their outermost surfaces. Raman experiments and numerical methods were conjugated to characterize the signatures from the active SiC normal modes and the vibrational density of states (VDOS). The Raman spectra of the nanopowders were marked by VDOS signals which correlate with the SiC amorphous fractions favoured by the high specific surfaces of the nanoparticles and their surface reconstruction. Quantitative interpretation of the experimental VDOS features, IR absorption and Raman scattering properties in nanosized SiC were carried out by means of numerical methods developed on SiC clusters with suitable structures and sizes.

1. Introduction

Nanocrystalline semiconductors are promising materials due to their versatile electronic and optical properties as opposed to those of bulk systems [1]. In this context, wide band gap SiC either in the form of thin films or containing appropriate doping agents (P, Er, N) is currently operating in different technical devices such as radiation sensors, solar cells, blue-light emitters and high-power electronics [2–4]. Recently, the synthesis of SiC nanoparticles has offered new opportunities to realize functional materials with promising nonlinear optical or electro-optical properties where the interface effects play a key role [5, 6]. An improvement of these properties

[5] Author to whom any correspondence should be addressed.

for potential applications requires rigorous control of the nanoparticle surfaces. However, with regard to the electronic and vibrational properties closely dependent on the microstructures of the materials [7–10], the nanoscale dimension and the interface effects are expected to induce a structural reconstruction of the outermost particle surfaces [11]. Thus, standard structural and vibrational experiments on nanosized systems and their interpretation within the theoretical framework developed for infinite crystals can suffer from some limitations. For example, the size and surface effects in nanocrystals modulate the chemical shift in NMR experiments [12] and, as reported below for SiC, the vibrational density of states (VDOS) dominates the Raman spectra of nanoparticles. This last behaviour contrasts with the structural investigations on the same systems by NMR (short-range order) and x-ray diffraction (XRD) [13], where the size effects contribute mainly to a line broadening of well resolved NMR or XRD lines. Furthermore, the features of VDOS bands induced by structural or chemical disorder, by the nanoscale size or by the surface reconstruction, cannot be stated easily. A relevant interpretation requires numerical simulations for the evaluation of the underlying structural and vibrational properties of nanoparticles. It is within such approaches that the effects of broken translation symmetry at the nanocrystal boundaries or the size-inducing electronic band structure and vibrational properties' changes [14] can be accounted for. However, these numerical methods are necessary to discriminate between the Raman spectrum contributions from VDOS and those from photoluminescence phenomena [15].

Thus, the present paper analyses the vibrational properties of SiC nanoparticles (np-SiC) by means of Raman spectroscopy. The main concern of the study is the low-wavenumber range of the Raman spectra where a vibrational density of states (VDOS) is present. The corresponding bands dominate the Raman signals from the as-formed SiC nanoparticles and overcome the lack of structural and vibrational information in these systems from SiC normal modes. Numerical simulations of the VDOS shapes are then developed on SiC clusters by using the semi-empirical parametric method (PM3) [16–18]. The theoretical VDOS bands allow a quantitative assignment of the experimental spectrum details. A close correlation is thus shown between the VDOS features and the amorphous SiC fractions induced by effective structural disorder in the nanoparticle cores or by its reconstructed surfaces.

2. Theoretical background of the numerical approach

Electron–phonon interactions play a major role on the optical and vibrational properties of nanosized systems. Indeed, the size dependence of the electron–phonon coupling in nanocrystals has been widely discussed for optical [19–23] and acoustic [24] phonon modes. In these systems, Raman and IR techniques are used to probe the structures from their active vibrational modes. The analysis of the corresponding spectra is based on the evaluation of the polarization tensor elements in the basis of vibration and electronic states.

From a simple approach concerning a molecular system, the electric component E_j of probing radiation interacts with valence electrons and induces a dipole moment:

$$\mu_i^{\mathrm{ex}} = \alpha_{ij} E_j \tag{1}$$

where $i, j = x, y, z$ represent the directions of the molecular referential frame and α_{ij} is the component of the polarizability tensor.

When the scattering process is involved between an initial $|m\rangle$ and a final $|n\rangle$ state of the system, the α_{ij} are expressed as a function of the matrix elements of the dipole component as follows:

$$[\alpha_{ij}]_{mn} \approx \frac{\langle m|\mu_i|n\rangle\langle n|\mu_j|m\rangle}{\hbar\omega_n - \hbar\omega_m} \approx \frac{\mu_{i,mn}\mu_{j,nm}}{\hbar\omega_{nm}} \tag{2}$$

where $\hbar\omega_{nm}$ is the energy difference between $|m\rangle$ and $|n\rangle$ states. The $\mu_{i,mn}$ represents the matrix element of ith component of the transition dipole moment between the states $|m\rangle$ and $|n\rangle$ which take into account both the electronic and the vibration degrees. The above elements of equation (2) are of particular interest because of the evaluation of the theoretical Raman and IR absorption spectra. Therefore, the scattered Raman intensity due to $|m\rangle$ to $|n\rangle$ transition is given by

$$I_{nm}(\omega) \approx I_0(\omega_0 - \omega_{mn})^4[\alpha_{ij}]_{mn}[\alpha_{ij}]^*_{mn} f(\omega) \tag{3}$$

where $f(\omega)$ represents a Lorentzian line shape taking into account the finite lifetime of the scattering and ω_0 represents the pulsation of the probing light.

The intensity of the IR absorption bands can also be defined from the transition dipole moment μ_{0n}, which couples the ground state $|0\rangle$ to excited ones $|n\rangle$ as follows:

$$I^{(\mathrm{IR})} \approx \sum_n \frac{\omega_{0n}|\mu_{0n}|^2}{\hbar\omega_{0n} - \hbar\omega_0}. \tag{4}$$

Theoretical calculations of IR absorption and Raman scattering including VDOS spectra can now be computed within the approach which models SiC clusters as was previously developed to analyse the photoluminescence features in np-SiC [15]. The cluster geometry is built by using the chemical bond lengths and angles involved in the cubic 3C-SiC and hexagonal 6H-SiC while the surface reconstruction can be simulated by allowing a geometric optimization of the cluster with the criterion of the lowest achieved energy. In this part of the simulations, the cluster is treated as a large molecule, for which vibration and electronic states are determined by quantum chemical codes. They are based on the self-consistent restricted (RHF) and unrestricted Hartree–Fock (UHF) semi-empirical PM3 method [16, 18]. The convergence is achieved when the difference between energies at iterations $(i + 1)$ and (i) is less than 10^{-7} eV. The optimization of surface chemical bonds was made by using the MM+ force field method [16].

A critical cluster size was determined with the criterion that the main features of the bulk-like spectra (absorption, vibration) are reproduced correctly. SiC clusters with 114 atoms were found relevant for this purpose. However, the central problem lies in the outermost cluster bonds. Their truncation modifies the optical band gap and alters both the optical and vibrational properties. According to our previous work on the photoluminescence phenomena [15] and experimental investigations [25], surface carbon atoms were bonded to ensure saturation of the cluster shell. The convergence criterion is then satisfactory fulfilled in the course of the computation process. The performed numerical simulations are hereafter used to describe mainly the VDOS spectra as well as the experimental results including the IR absorption.

3. Experimental details

3.1. Synthesis

Nanopowders were synthesized by CO_2-laser pyrolysis of a gaseous mixture (silane, acetylene) following the process described elsewhere [15, 25, 26]. Quasi-stoichiometric nanoparticles (np-SiC) were obtained under suitable experimental conditions (flux of the gaseous reactants, time duration of their chemical decomposition in the reaction chamber and the laser power). Then, two np-SiC samples were selected; these will be referred to as SiC229 and SiC238. Below, we summarize the main results on the nanoparticles' stoichiometry, morphology and structure.

3.2. Composition

The elemental chemical analysis was performed and reveals a small fraction of excess carbon of about 2%; i.e. atomic ratio C/Si = 1.02 in the investigated samples. A confirmation was obtained from precise electron paramagnetic resonance investigations through the concentration of dangling bonds brought by carbon atoms in comparison to a reference sample [13]. The excess of carbon has indeed a natural tendency to migrate at the outermost particle surfaces.

3.3. Morphology

Transmission electron microscopy (TEM) was used to characterize the particle shapes, sizes and the boundary features. Typical morphologies and organization of the SiC229 nanoparticles are illustrated in figure 1 by using high-resolution TEM experiments. For this sample, the nanoparticle exhibits an average diameter about 10 nm and consists of several small nanocrystals (5 nm in diameter) separated by stacking faults at the nanocrystal boundaries. In the as-formed nanopowders (figure 1(a)), the external particle surfaces exhibit diffused boundaries because of structural disorder and a reconstruction at nanocrystal interfaces. For the nanopowder annealed at 1400 °C, figure 1(b) illustrates the improvement of the crystalline order in the nanoparticles. Similar investigations by TEM on the SiC238 sample showed that the nanoparticles have spherical shapes and monodisperse diameters of the order of 25 nm. In this sample, the entire nanoparticle consists of a single crystallite with relatively better crystalline order than in the SiC229 sample.

3.4. Structure

The investigations performed were carried out by x-ray diffraction (XRD) and by ^{29}Si solid-state NMR. In both samples, the NMR results were consistent with crystal structures which belong to the cubic (3C-SiC) and hexagonal (6H-SiC) polytypes. The amorphous fraction, which can result from stacking faults, disorder or from surface reconstruction, was also evaluated from NMR experiments [15]. In the SiC238 sample, a low amorphous fraction about 10% was determined in contrast to a high fraction (∼80%) in the SiC229 sample. This is a consequence of the low nanocrystal dimensions and the structural disorder at the nanocrystal boundaries. However, an improvement of the crystalline order, without a net modification of the particle size, can be achieved by suitable thermal treatments performed by heating the sample under argon atmosphere for one hour at temperatures up to 1400 °C.

In the following, beyond a preliminary analysis of the IR absorption spectra of the SiC samples, the vibrational properties were investigated by means of a confocal micro-Raman spectrometer coupled with an argon–krypton laser. All the experiments were realized by selecting 514 nm radiation with a fixed power at the sample of about 0.8 mW μm^{-2}. The main goal is to clarify the low-wavenumber peculiarities of the Raman spectra marked by the phonon density of states in the np-SiC samples.

4. Experimental results and discussion

4.1. Raman spectra and IR absorption of the as-formed SiC nanopowders

4.1.1. Raman investigations. The experimental spectra are reported in figure 2 on a large wavenumber range. The weak or even absent Raman bands from the SiC normal modes in, respectively, SiC238 and SiC229 samples, is an intriguing fact. The only well resolved signals correspond to the known carbon Raman-active modes reported in graphite, glassy carbon or in

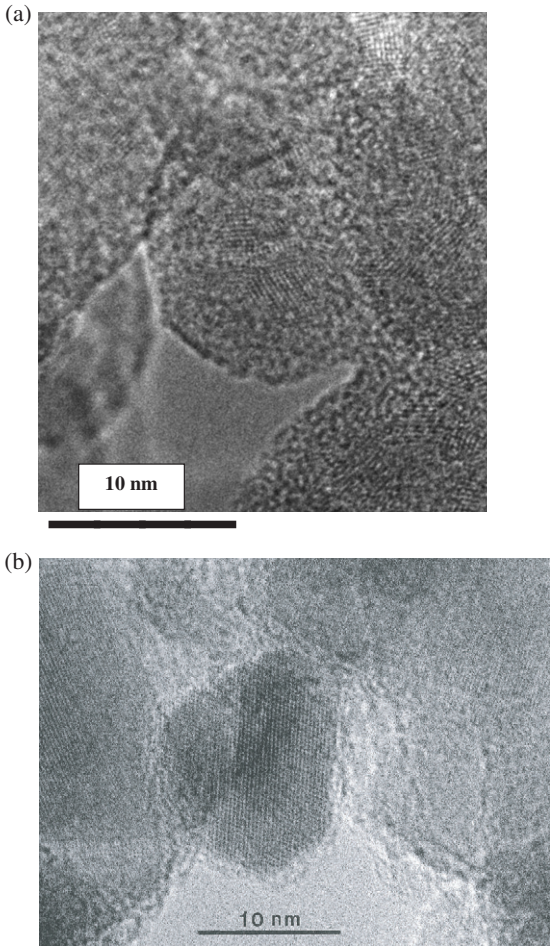

Figure 1. High-resolution transmission electron microscopy images in the SiC229 nanopowder; (a) as-formed sample and (b) sample annealed at 1400 °C. An improved crystalline order in the nanoparticles is evidenced by the annealing treatment.

diamond-like carbon structure [25]. These observations correlate with the elemental chemical analysis which shows about 2% of carbon excess in both samples. The scattering efficiency of this low excess seems so high as to screen the contributions from the Raman-active mode of SiC. With regard to the high specific surfaces of these nanopowders, a carbon-rich phase located at the outermost particle surfaces can account for the features of the Raman spectra in the as-formed powders. In particular, the main resolved bands from the SiC238 sample are attributed to surface carbon atoms with sp^3 and sp^2 hybridization which give rise to the L1 ($\sim$1345 cm^{-1}) and L2 ($\sim$1596 cm^{-1}) bands. In the sample SiC229, the Raman spectrum consists of smeared broad bands with only weak singularities located in the wavenumber range where the L1 and L2 bands are expected.

4.1.2. IR spectra in the as-formed nanopowders. The lack of information from the Raman spectra and in general on the normal modes from SiC structures can be partially explained by IR absorption. By using the numerical approaches of section 2, the theoretical IR spectra were computed for different cluster sizes (figure 3(a)) and a comparison with experiments is reported in figure 3(b) for the SiC229 sample. A bulk-like spectrum was satisfactory obtained for an optimal cluster size about 1.1 nm in diameter. However, to account for the experimental

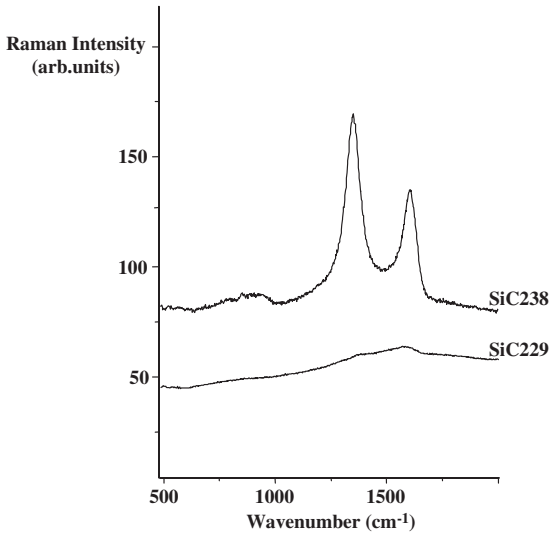

Figure 2. Raman spectra in the as-formed SiC nanopowders dominated by signatures from normal modes of the low carbon in excess (C/Si = 1.02). Carbon Raman bands with sp^3 and sp^2 bonding are associated respectively to the L1 (1345 cm^{-1}) and L2 (1596 cm^{-1}) bands. Only a weak SiC Raman band in the wavenumber range 700–1000 cm^{-1} seems to hold in the SiC238 sample.

IR results, it was necessary to achieve a superposition of calculation runs performed on two 1.1 nm SiC clusters; i.e. an amorphous-like and a cubic 3C-SiC cluster. The pertinence of the numerical approach to reproduce the experimental IR spectra (figure 3(b)) with suitable cluster about 1.1 nm was thus demonstrated. As discussed hereafter, this numerical procedure offers a consistent description of the vibrational properties of nanosized SiC through their VDOS signatures.

4.2. VDOS spectra versus the nanocrystal size and the amorphous fraction of the nanoparticles

The Raman spectra were recorded in the same conditions for the as-formed nanopowders and annealed ones at 1200 and 1400 °C (figures 4, 5). The relevant scattering details from SiC consist of two main structured bands located in the ranges (100, 600 cm^{-1}) and (700, 1000 cm^{-1}). They are respectively associated to VDOS from the acoustic and optic modes of the SiC structures. The main difference between the SiC229 sample (nanoparticles composed of several nanocrystals) and SiC238 (nanoparticle as a single nanocrystal) lies in the enhanced intensity of the VDOS signals in SiC229. However, annealing at 1400 °C gave rise in both samples to better resolved LO and TO SiC vibration modes as well as the suppression of the VDOS signals (figures 4(c), 5(c)). A quantitative analysis of the experimental spectra was undertaken by the numerical approach of section 2. Theoretical spectra were obtained by using SiC clusters with different diameters (figure 6) and with cubic, hexagonal and amorphous structures (figure 7); the diameter was fixed at 1.1 nm. The numerical results shed light on the different details resolved in the VDOS spectrum shapes.

On the one hand, the optical modes hold within the spectral range 700–1000 cm^{-1} while acoustic mode contributions are located in the 140–650 cm^{-1} wavenumber range in agreement with previous reports on SiC polytypes [27–30]. Also, the calculated VDOS spectra for amorphous clusters seem closer to the experimental curves obtained on the as-

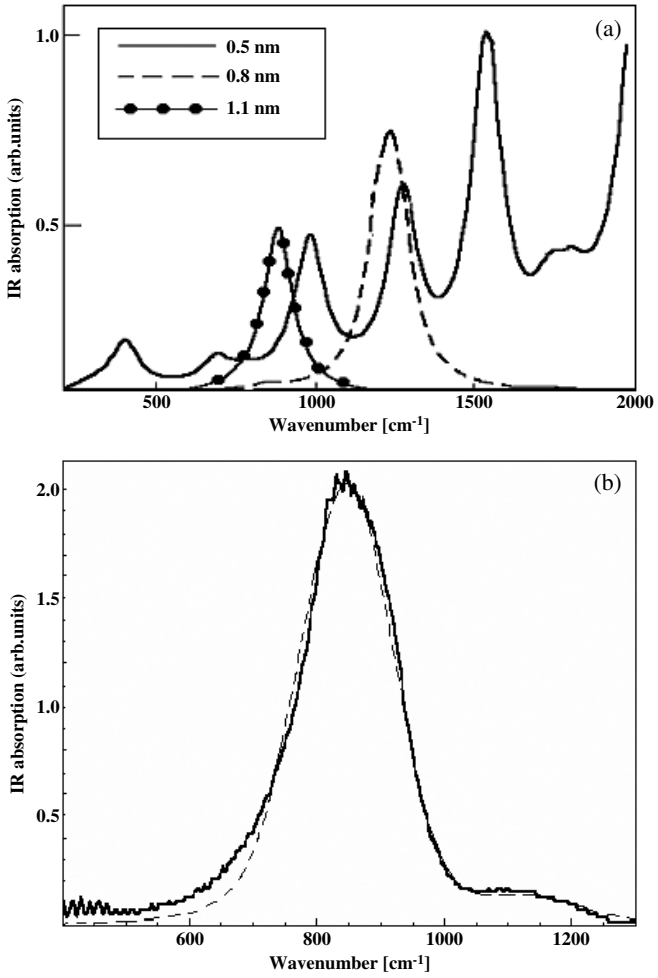

Figure 3. (a) Calculated IR absorption spectra for cubic SiC clusters with different diameters (0.5 nm: continuous line, 0.8 nm: dashed line and 1.1 nm: dotted line). Calculations from the cluster with 1.1 nm diameter give a typical shape of the absorption spectrum from the bulk SiC. (b) Experimental IR spectrum in SiC229 nanopowder (continuous line) and a calculated shape (dashed line) using contributions from two SiC clusters (1.1 nm) with the cubic and amorphous arrangements.

formed nanopowders (figures 4(a), 5(a)). This suggests that the main contribution to the experimental VDOS comes from the amorphous fractions of the nanoparticles in agreement with the structural characterizations by NMR.

On the other hand, in the performed experiments, the size effects did not match the conclusions of former works [31–35]. In these references, Raman bands from normal modes were indeed observed even if the nanocrystalline size drastically modifies their line-shape. This behaviour is attributed to a spatial confinement of phonons following the same principle which monitors the movement of electrons in nanostructures. For both vibrational and electronic aspects, the reference length scale can be defined by the exciton Bohr radius. This criterion is—*a priori*—fulfilled in the investigated SiC229 sample with an average nanocrystal diameter about 5 nm, i.e. less than the exciton Bohr diameter in bulk SiC. Consequently, one expects a

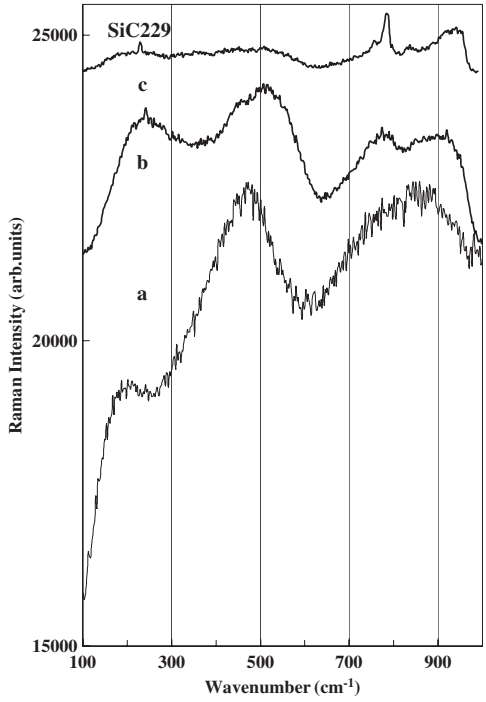

Figure 4. Raman scattering signal in SiC229 sample for the as-formed nanopowders (a) and after annealing at 1200 °C (b) and 1400 °C (c). SiC Raman bands associated to TO and LO active modes are well resolved after annealing at 1400 °C.

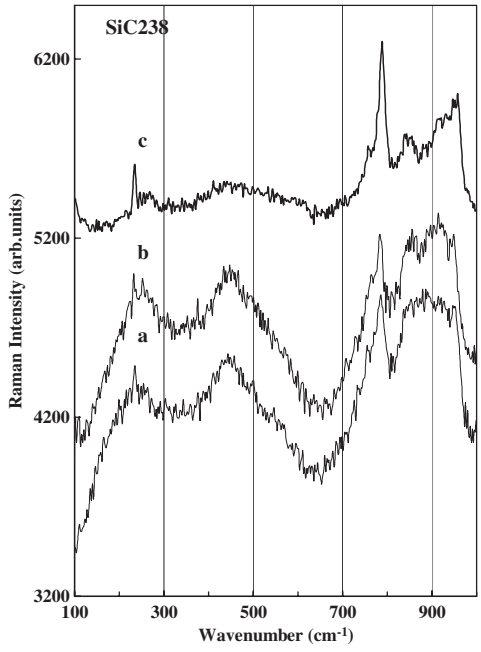

Figure 5. Low-frequency Raman spectra of SiC238 nanopowders versus annealing. (a) As-formed powder, (b) annealing at 1200 °C and (c) annealing at 1400 °C. SiC Raman active modes at 795 and 967 cm^{-1} are well resolved after annealing at 1400 °C.

widening of Raman bands from the SiC normal modes. However, the performed experiments and the numerical simulations showed only VDOS signatures mainly correlated with the amorphous SiC fractions. The size effects revealed from the present work are mainly limited to the abnormally enhanced intensity of the VDOS signal in SiC229. Beyond effective amorphous

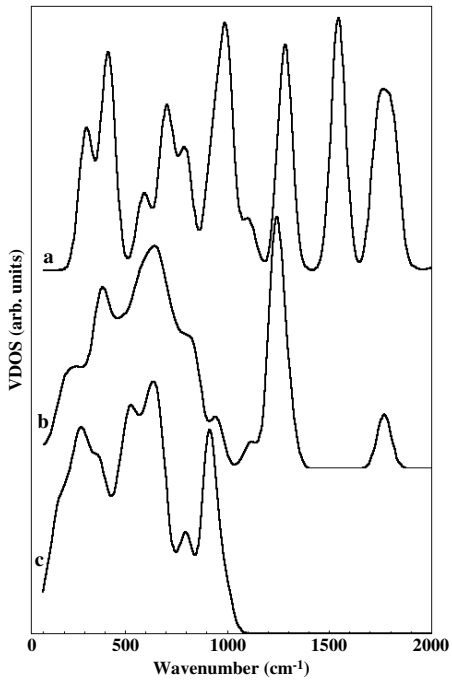

Figure 6. Calculated vibrational density of states (VDOS) in SiC cluster with cubic structure for different cluster sizes; (a) 0.5 nm, (b) 0.8 nm and (c) 1.1 nm.

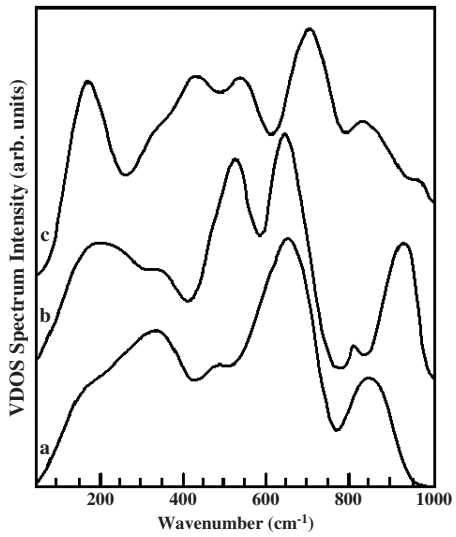

Figure 7. Calculated vibrational density of states in the low-wavenumber range for SiC nanoclusters (1.1 nm) with cubic SiC (a), hexagonal (b) and amorphous (c) arrangements obtained by a full geometry optimization of the Si–C bonds.

structures, the experimental VDOS is understood by the presence of crystallites with small sizes, i.e. a high area of interfaces. Such microstructures exhibit structural reconstruction and relaxation which contribute to VDOS signatures in the SiC nanopowders.

5. Conclusion

Raman experiments were performed on SiC nanoparticles with different sizes and structures. The analysis of Raman spectra has pointed out that the vibrational properties in these nanosized materials give rise to enhanced VDOS signatures. Numerical simulations of the VDOS bands

were carried out using different cluster sizes and local structures. The relevant theoretical shapes, which agree with the experimental spectra, were obtained on amorphous clusters. The main contributions to the VDOS are induced by SiC amorphous fractions within the nanoparticles and they correlate with nanocrystal sizes in the investigated samples which favour the occurrence of surface reconstruction and relaxation. In fact, this work demonstrates the possibility to probe the physical organization of the SiC nanoparticles from their VDOS signatures.

Acknowledgments

We are grateful to Dr J Vicens (LERMAT-Caen-France) for the TEM image on the as-formed SiC229 sample and to Dr N Herlin-Boime (CEA-Saclay-France) for the synthesis of the SiC229 sample. Katya Tebeleva is acknowledged for English text corrections.

References

[1] Manna L, Scher E C and Alivisatos A P 2000 *J. Am. Chem. Soc* **122** 12700 and references therein
[2] Desalvo A, Giorgis F, Pirri C F, Tresso E, Rava P, Galloni R, Rizzoli R and Summonte C 1997 *J. Appl. Phys.* **81** 7973
[3] Vonsovici A, Reed G T and Evans A G R 2000 *Mater. Sci. Semicond. Process.* **3** 367
[4] Tessler L R 1999 *Solid State Commun.* **111** 193
[5] Bouclé J, Kassiba A, Makowska-Janusik M, Sanetra J, Herlin-Boime N, Bulou A and Kodjikian S 2005 *Opt. Commun.* **246** 415
[6] Wu X L, Fan J Y, Qiu T, Yang X, Siu G G and Chu P K 2005 *Phys. Rev. Lett.* **94** 026102
[7] Hill N A and Whaley K B 1995 *Phys. Rev. Lett.* **75** 1130
[8] Mews A, Kadavanich A V, Banin U and Alivisatos A P 1996 *Phys. Rev.* B **53** 13242
[9] Kagam C R, Murray C B, Nirmal M and Bawendi M G 1995 *Phys. Rev. Lett.* **76** 1517
[10] Noris D J and Bawendi M G 1996 *Phys. Rev.* B **53** 1933
[11] Dai Z R, Sun S and Wang Z L 2002 *Surf. Sci.* **505** 325
[12] Tomaselli M, Yarger J L, Bruchez M, Havlin R H, deGraw D, Pines A and Alivisatos A P 1999 *J. Chem. Phys.* **110** 8861
[13] Charpentier S, Kassiba A, Emery J and Cauchetier M 1999 *J. Phys.: Condens. Matter* **11** 4887
[14] Lin S-Y and Chang S T 1998 *J. Phys. Chem. Solids* **59** 1399
[15] Kassiba A, Makowska-Janusik M, Bouclé J, Bardeau J F, Bulou A and Herlin-Boime N 2002 *Phys. Rev.* B **66** 155317
[16] HyperChem^{TM} 1999 *Computational Chemistry* (Hypercube)
[17] Weiner S J, Kollman P A, Case D A, Ghio U C, Alagona G, Profeta S Jr and Weiner P 1984 *J. Am. Chem. Soc.* **106** 765
[18] Weiner S J, Kollman P A, Nguyen D T and Case D A 1986 *J. Comput. Chem.* **7** 230
[19] Schmit-Rink S, Miller D A and Chemla D S 1987 *Phys. Rev.* B **35** 8113
[20] Klein M C, Hache F, Ricard D and Flytzanis C 1990 *Phys. Rev.* B **42** 11123
[21] Efros A L, Ekimov A I, Kozlowski F and Petrova-Koch V 1991 *Solid State Commun.* **78** 853
[22] Tanaka A, Onari S and Arai T 1992 *Phys. Rev.* B **45** 6587
[23] Shiang J J, Risbug S H and Alivisatos A P 1993 *J. Chem. Phys.* **98** 8432
[24] Itoh T, Ekimov A I, Gourdon C, Efros A L and Rosen M 1995 *Phys. Rev. Lett.* **7** 1645
[25] Charpentier S, Kassiba A, Bulou A, Monthioux M and Cauchetier M 1999 *Eur. Phys. J A.P* **8** 11
[26] Kassiba A, Makowska-Janusik M, Bouclé J, Bardeau J-F, Bulou A, Herlin N, Mayne M and Armand X 2002 *Diamond Relat. Mater.* **11** 1243
[27] Zhang H and Xu Z 2002 *Opt. Mater.* **20** 177
[28] Lucovsky G and Pollard W B 1984 *The Physics of Hydrogenated Amorphous Silicon* (Berlin: Springer)
[29] Lin S Y and Chang S T 1998 *J. Phys. Chem. Solids* **59** 1399
[30] Hofmann M, Zywietz A, Karch K and Bechstedt F 1994 *Phys. Rev.* B **50** 13401
[31] Norris D J and Bawendi M G 1996 *Phys. Rev.* B **53** 16338
[32] Gammon D, Snow E S, Shanabrook B V, Katze D S and Park D 1996 *Phys. Rev. Lett.* **76** 3005
[33] Kosacki I, Suzuki T, Anderson H U and Colomban Ph 2002 *Solid State Ion.* **149** 99
[34] Ma G, Shen Z, Huang W and Shi J 2002 *Phys. Lett.* A **229** 581
[35] Spanier I E, Robinson R D, Zhang F, Chan S-W and Herman I P 2001 *Phys. Rev.* B **64** 245–407